Available online at www.sciencedirect.com

SCIENCE DIRECT®

Journal of Molecular Catalysis A: Chemical 202 (2003) 73–85

JOURNAL OF MOLECULAR CATALYSIS A: CHEMICAL

www.elsevier.com/locate/molcata

Photocatalytic reduction of Se(VI) in aqueous solutions in UV/TiO_2 system: importance of optimum ratio of reactants on TiO_2 surface

Timothy T.Y. Tan, Donia Beydoun, Rose Amal*

Centre for Particle and Catalyst Technologies, School of Chemical Engineering and Industrial Chemistry, University of New South Wales, Sydney, NSW 2052, Australia

Received 20 September 2002; accepted 12 March 2003

Abstract

This study investigates the effect of pH, initial concentrations of formic acid and selenate (Se(VI)) ions on the UV/TiO_2 reduction of Se(VI) ions. The adsorption of Se(VI) and formate ions onto TiO_2 surface was essential before the Se(VI) ions could be photoreduced to elemental selenium (Se). The elemental Se was further reduced to hydrogen selenide (H_2Se) once the Se(VI) ions were exhausted from the solution. An interesting finding arisen from the current investigation is that the optimum reduction rate of Se(VI) was closely correlated to the molar adsorption ratio of 3:1 of formate-to-selenate on the TiO_2 surface. This ratio also corresponded to the stoichiometry of the overall reaction which involved 3 mol of formate ions reacting with 1 mol of Se(VI). It was postulated that this ratio provided the highest efficiency in capturing the photogenerated holes and electrons, hence resulting in optimum Se(VI) photoreduction. The optimum molar adsorption ratio could be achieved by manipulating the initial pH, initial solute concentration and the order of which the solutes were adsorbed.

Keywords: Selenate; Photocatalytic reduction; Formate; Stoichiometry

1. Introduction

Selenium (Se) exists in natural waterways as a result of seleniferous soil. It is an important trace nutrient for both human and animals [1,2]. A dietary intake of about 50 μg per day is suggested for women and 70 μg per day is suggested for men for the daily nutritional need [3]. However, when consumed consistently at about 10 times the daily requirement, Se and its ions accumulate in the body and become toxic. They are known to cause deformities and death in extreme case [4]. In recent years, human activities such as smelting and coal-power generation industries, mining and agricultural drainage have increased Se contamination significantly [5]. Hence, many investigations on the interaction of Se compounds with the ecosystems have been carried out. These investigations include the interactions of Se compounds with lake and wetland sediments [6,7], speciation of Se compounds with variation of chemical potential and pH of the environment [8], and the adsorption of Se compounds at particulate interfaces [9].

Se can exist as mobile ions, such as selenate (Se(VI), SeO_4^{2-}), selenite (Se(IV), SeO_3^{2-}) and their protonated anions ($HSeO_4^-$, $HSeO_3^-$). These are the most common Se species found in wastewater. Se can

* Corresponding author. Tel.: +61-2-9385-4361; fax: +61-2-9385-5966.
E-mail address: r.amal@unsw.edu.au (R. Amal).

1381-1169/03/$ – see front matter © 2003 Elsevier Science B.V. All rights reserved.
doi:10.1016/S1381-1169(03)00205-X

also exist in a variety of compounds such as insoluble oxides/hydroxides, organoselenium compounds and selenides [10]. The toxicity of Se compounds is related to their oxidation states: Se(VI) is more mobile and stable towards reduction than Se(IV), hence harmful and difficult to be removed from wastewater [8].

The present maximum contaminant level for Se for US drinking water standard is 50 μg/l while Australia has a lower standard at 10 μg/l [11]. In Japan, the effluent standard for Se is 100 μg/l [12,13]. Such stringent standards have resulted in widespread interests in the removal of Se compounds from water and wastewaters. Removal methods include physical, biological and chemical means. Physical removal methods involve the use of adsorption [14], ion exchange [15] and membrane processes [16,17]. These methods simply concentrate the Se compounds and hence their subsequent disposal remains a major problem. Biological removal involves the reduction of oxidised Se forms, such as selenate and selenite to elemental Se by bacteria [18–20]. Some problems associated with biological reduction include the difficulty in promoting growth of the bacteria due to the inhibitory effect of the elemental Se formed [21]. Chemical reduction of oxidised forms of Se has been achieved using ferrous hydroxide in a patented process [22–24] as well as by using zero-valence iron [25]. These processes usually involve a high chemical cost.

Photo-assisted reduction using semiconductor particles as catalysts is now an emerging and promising technology. Of all semiconductors, titanium dioxide has been widely investigated in such photocatalytic processes [26–28]. Titanium dioxide is a popular photocatalyst due to its high stability, non-toxicity and its ability to be reused after recycle from the treated water stream [29].

The ability of titanium dioxide to function as a photocatalyst arises from its semiconducting properties. Illumination of semiconductor particles with electromagnetic radiation with energy greater than their band-gap results in the promotion of an electron from the valence band (VB) to the conduction band (CB). This generates pairs of electrons (e^-) and holes (h^+) in the CB and VB, respectively. The CB becomes electron-rich and hence possesses a reducing ability while the VB hole is deficient of electrons, hence possesses an oxidising ability [30]. In the context of Se(VI) or Se(IV) reduction, the CB electron is transferred to either the adsorbed Se(VI) or Se(IV) species, reducing them to elemental Se. In the presence of dissolved oxygen in the solution, the dissolved oxygen molecules are reduced to superoxide radicals while VB holes can accept electrons from water, forming highly oxidising hydroxyl radicals [31]. Organic species present in solution may react directly with the holes or hydroxyl radicals, depending on their concentration in the solutions. Generally, at a high organic concentration, direct oxidation by the holes is more dominant [32].

The use of photocatalytic reduction to recover precious metals such as silver [33] and platinum [34] has been investigated. The photocatalytic reduction and removal of toxic pollutants such as chromate [35,36], nitrate [37,38] and heavy metals such as cadmium and zinc [39,40] has also been studied. The adsorption of these heavy metal ions as well as the presence and adsorption of organics on the photocatalyst surface have been identified as being essential in achieving a high photoreduction rate [41]. This was attributed to the synergistic effect of holes scavenging by the organics (the reductants) and electrons scavenging by the heavy metal ions, preventing e^-–h^+ recombination.

The research carried out on the photocatalytic reduction of Se(VI) or Se(IV) species using titanium dioxide as the catalyst is limited. Sanuki et al. [12,13] have investigated such photocatalytic reduction and found that the adsorption of Se(VI) or Se(IV) species onto titanium dioxide and the presence of suitable hole scavengers were significant for an effective reduction process. In addition, the adsorption of Se(IV) onto the TiO_2 surface and the rate of Se(IV) reduction were both found to be higher than those of Se(VI). The presence of sulfate ions in the solution was found to depress Se(VI) or Se(IV) reduction rates. Kikuchi and Sakamoto [42] have also investigated this process and have proposed that when all Se(VI) or Se(IV) ions were reduced to amorphous Se, no more species in the solution could capture the electrons from the TiO_2 surface. This raised the conduction band and further reduced the amorphous Se to hydrogen selenide (H_2Se) gas [42].

In the present paper, the effect of various experimental parameters, such as pH, initial concentrations of organic additives (formic acid) and Se(VI) ions on the photocatalytic reduction of Se(VI) ions was studied. The study focuses on investigating the synergistic

and competitive effects of which the presence of formate and selenate ions on the TiO_2 surface have on the photocatalytic reduction of selenate ions.

2. Experimental

2.1. Catalyst and reagent

Degussa P25 titanium dioxide was used as the photocatalyst. It is composed of approximately 70% anatase and 30% rutile, and has a specific surface area of about 59 m^2/g obtained from BET analysis. The primary particle is 20–30 nm in diameter. Sodium selenate was used as the Se source and formic acid (77%) as the organic reductant (hole scavenger). Copper(II) sulfate and sodium hydroxide were used to trap hydrogen selenide gas which escaped from the reactor. Sodium hydroxide and perchloric acid were used to adjust the pH. Deionised pure water was used for the preparation of all solutions. For colorimetric analysis of Se(IV), 2,3-diaminonaphthalene (DAN), cyclohexane, hydroxylamine chlorohydrate and EDTA were used.

2.2. Apparatus and procedure

The schematic of the experimental set-up is shown in Fig. 1. It consists of a cylindrical glass reactor of 1.2 l capacity with a side quartz-window through which UV was irradiated from a 200 W Mercury lamp (Oriel 66001-373). Gas exhausted from the reactor was introduced into two traps in series, containing 5×10^{-3} M $CuSO_4$ and 0.1 M NaOH, respectively to remove possible toxic hydrogen selenide gas generated from the reduction process. The solution in the reactor was agitated by the combined action of air or nitrogen bubbling (1.5 l/min) and magnetic stirrer (250 rpm). The required Se(VI) ions (10–40 ppm Se) and formic acid (20–600 ppmC) (ppmC: parts per million carbon) concentrations were then made into a test solution of volume 0.5 or 1 l, followed by pH adjustment and the addition of titanium dioxide powder (1.1 gTiO_2/l). The reported pH of the experiments was the one obtained after the addition of TiO_2. The suspension was stirred for 30 min before illumination by the UV-radiation. The photon flux into the reactor was determined to be 3.8 μmol photon/s by chemical actinometry [43,44].

2.3. Adsorption data and isotherm determination of se ions on TiO_2

Solutions containing sodium selenate with Se concentration ranging from 2 to 80 ppm (0.025–1 mM) and formic acid concentration ranging from 20 to 500 ppmC (1.67–42 mMC) were subjected to adsorption isotherm analysis. 1 l of these solutions was put

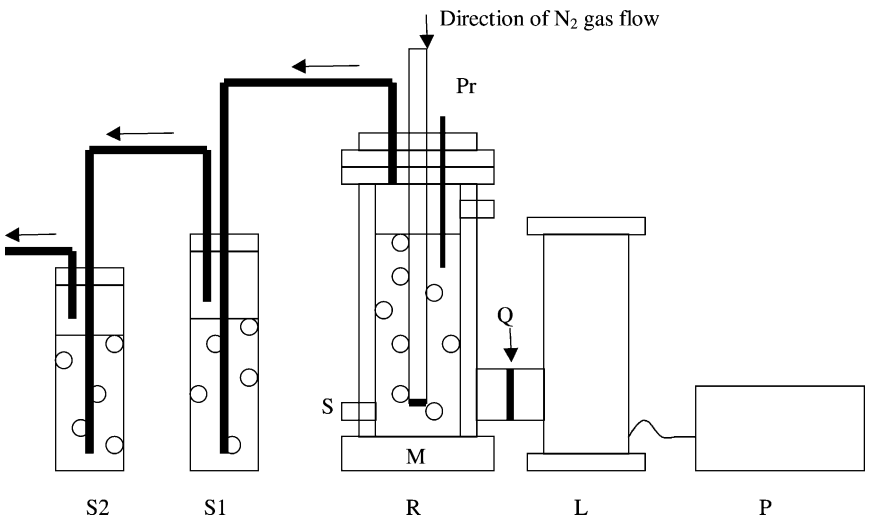

Fig. 1. Schematic illustration of the experimental set-up. P: power supply, L: lamp housing with Hg lamp, R: glass reactor, M: magnetic stirrer, Q: quartz-window, S: sampling port, Pr: pH probe, S1: $CuSO_4$ scrubber for H_2Se, S2: NaOH scrubber for H_2Se.

in the reactor mixed with 1.1 gTiO_2 powder added and stirred continuously with nitrogen bubbling for 30 min at atmospheric conditions. From the kinetics of adsorption, it was found that 15 min was sufficient to reach adsorption equilibrium. After the 30 min, the suspension was filtered, the concentration of Se and the total organic carbon (TOC) in the filtrate were analysed. The amount of Se or formic acid adsorbed onto the TiO_2 particles was calculated from the difference between the initial and residual Se(VI) ions or formic acid concentrations. Separate experiments verified that the amount Se(VI) or formic acid adsorbed onto the reactor surface was insignificant.

2.4. Analysis

All samples were withdrawn from the sample port using a syringe and then immediately filtered using 0.22 μm Millipore membrane by Millipore. The total Se concentration (Se(VI)) in the filtrate was determined by Varian Induced Coupled Plasma-Atomic Emission Spectroscopy (ICP-AES) while Se(IV) was determined colorimetrically by methods developed by Holtzclaw et al. [45]. The amount of H_2Se generated was determined by analysing the amount of Cu(II) remaining in the trap using Varian ICP-AES. The formic acid concentration was determined by analysing the total organic carbon in the solution using a Shimadzu TOC-5000 A analyser. The amount of Se deposited on titanium dioxide was determined by digesting the metals using concentrated nitric acid and analyzing the digested Se ions by Varian ICP-AES. Zeta potential and particle size of the TiO_2 suspensions were determined by electrophoresis and Photon Correlation Spectroscopy (PCS) techniques, respectively using the Brookhaven 3-in-1 system. The surface area of Degussa P25 was obtained by Micromeritics ASAP 2000 BET surface analyser.

3. Results and discussion

3.1. Adsorption studies

Prior to the adsorption studies, the point of zero charge (pH_{zpc}) of Degussa P-25 TiO_2 was determined to be 5.6. The individual adsorption isotherms of Se(VI) and formate ions onto the TiO_2 surface were then investigated. The adsorption isotherm of Se(VI) conforms to the trend of multi-layer adsorption for a non-porous particle, which can be described by the Brunauer–Emmett–Teller (BET) multi-layer adsorption isotherm model (Eq. (1)). This is shown in Fig. 2. This model assumes that the layers beyond the first have equal energies of adsorption [46]:

$$q_e = \frac{BC_e Q_0}{(C_e - C_s)[1 + (B-1)(C_e/C_s)]} \quad (1)$$

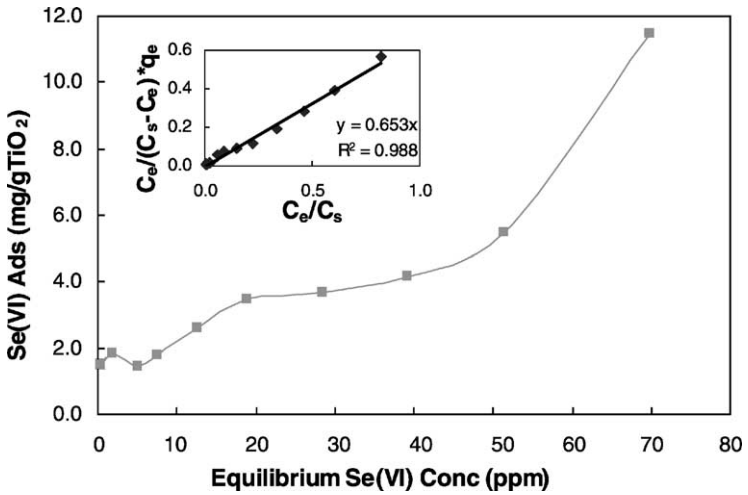

Fig. 2. Adsorption isotherm of Se(VI). Experimental conditions: pH 3.5, 1 l test solution, 1.1 gTiO_2/l, N_2 purging, 293 K. Insert: linearised BET model plot.

where C_s is the saturation concentration, q_e the amount of solute adsorbed per unit weight of adsorbent, C_e the residual solute concentration at equilibrium, B the constant expressive of energy of adsorption and Q_0 is the solid-phase concentration corresponding to complete coverage of available sites.

By linearising Eq. (1), a plot of $C_e/(C_e - C_s)q_e$ versus C_e/C_s should yield a straight line if the adsorption isotherm obtained follows the BET model. The insert in Fig. 2 shows that the isotherm fits well to the BET model with the sum of residual square (R^2) of 0.988.

The adsorption isotherm of formic acid is shown in Fig. 3. It follows the Langmuir adsorption isotherm which can be expressed as:

$$\frac{C_F}{C_{F-m}} = \frac{K_F C_e}{1 + K_F C_e} \quad (2)$$

where $C_{F\text{-}m}$ is the monolayer saturation concentration, C_F the amount of solute adsorbed per unit weight of adsorbent, C_e the residual solute concentration at equilibrium and K_F is the adsorption constant.

Comparing the adsorption isotherms in Figs. 2 and 3, the adsorption of formic acid onto TiO_2 was not as significant as Se(VI) adsorption at pH 3.5. Only 3.0 mgC/gTiO_2 of formate ions were adsorbed when the amount of formic acid added into 1.1 g/l TiO_2 was 300 mgC. However, when the amount of Se(VI) added in solution was 70 mg, about 11.3 mg/gTiO_2 of Se(VI) ions were adsorbed, forming multi-layers of Se(VI) ions. This indicated a higher affinity of Se(VI) ions to the TiO_2 surface, which. This could be attributed to the higher negative charge of Se(VI) ions.

The competitive adsorption of Se(VI) and formic acid on TiO_2 at various pH values and initial solute concentrations were also investigated. Fig. 4 shows the adsorption of Se(VI) ions onto TiO_2 particles in the absence and presence of formic acid at various pH values. The adsorption of Se(VI) ions was found to reach equilibrium within 1–2 min. In the investigated pH range of 1.5–6.5, sodium selenate (pK_d = 0.02) [47] was completely dissociated while formic acid (pK_a = 3.77) [48] was increasingly ionised to the negatively-charged formate ions as the pH increased. Se(VI) is mostly present as the negatively-charged SeO_4^{2-} ions at pH 2 and above (H_2SeO_4, $pK_a = -2.01 \pm 0.06$ and $HSeO_4^-$, $pK_a = 1.8 \pm 0.1$) [47]. The negatively-charged nature of the selenate and formate ions enabled the adsorption of these ions onto the positively-charged TiO_2 below its pH_{zpc}.

Also shown in Fig. 4, at pH 1.5 and 2.5, the amount of Se(VI) ions adsorbed was not affected by the presence of formic acid. This was due to the low formate ionisation at high H^+ concentration (low pH). As the pH increased, the amount of Se(VI) ions adsorbed decreased since the TiO_2 surface became less positively charged. At pH higher than 2.5 and in the presence

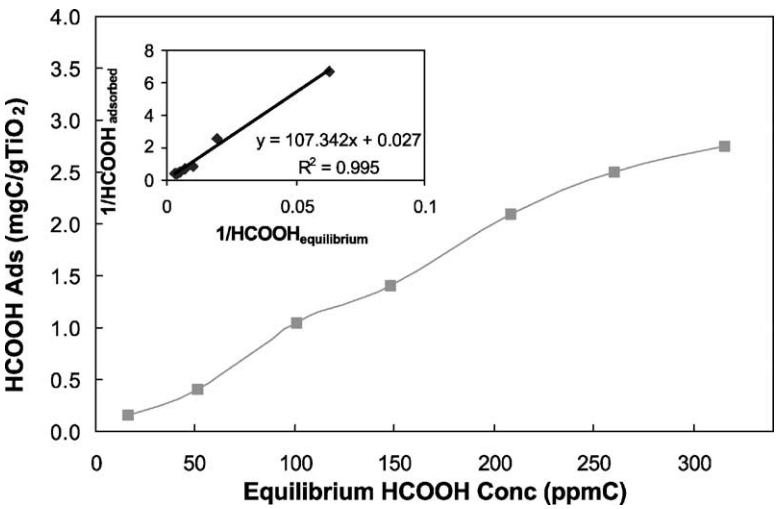

Fig. 3. Adsorption isotherm of HCOOH. Experimental conditions: pH 3.5, 1 l test solution, 1.1 gTiO_2/l, N_2 purging, 293 K. Insert: linearised LH adsorption model plot.

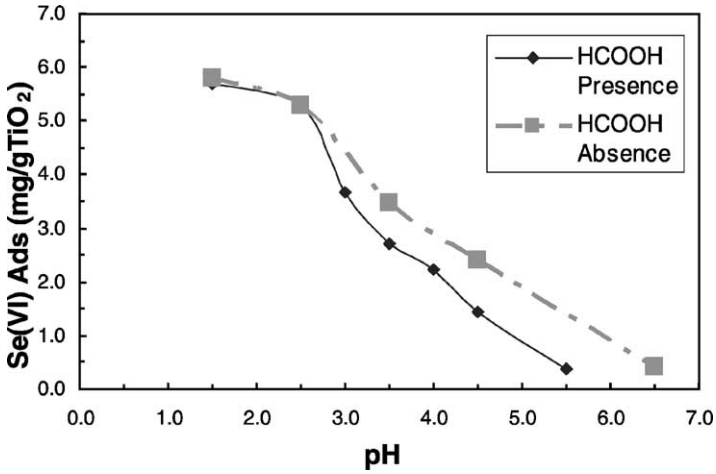

Fig. 4. Effect of pH on Se(VI) adsorption. Experimental conditions: 1 l test solution, $[Se(VI)]_0$: 20 ppm (0.256 mM), $[HCOOH]_0$: 100 ppmC (8.3 mMC), 1.1 gTiO_2/l, N_2 purging, 293 K.

of formic acid, less Se(VI) ions were adsorbed onto TiO_2 at pH higher than 2.5, indicating a competition between the two negatively-charged Se(VI) and formate ions for the positively-charged adsorption sites on the TiO_2 particles. As the pH was raised, formate ions concentration increased due to a greater extent of formic acid ionisation, formate ions adsorption increased, which further depressed the adsorption of Se(VI) ions. From pH 5.5–6.5, once the pH_{zpc} of TiO_2 was reached, very little Se(VI) ions were adsorbed.

The competitive adsorption of the Se(VI) and formate ions at various pH is further depicted in Fig. 5. Besides further consolidating the finding that increasing pH resulted in the decreased adsorption of Se(VI) but the increased adsorption of formate ions, the data from Fig. 5 also enables the determination of the

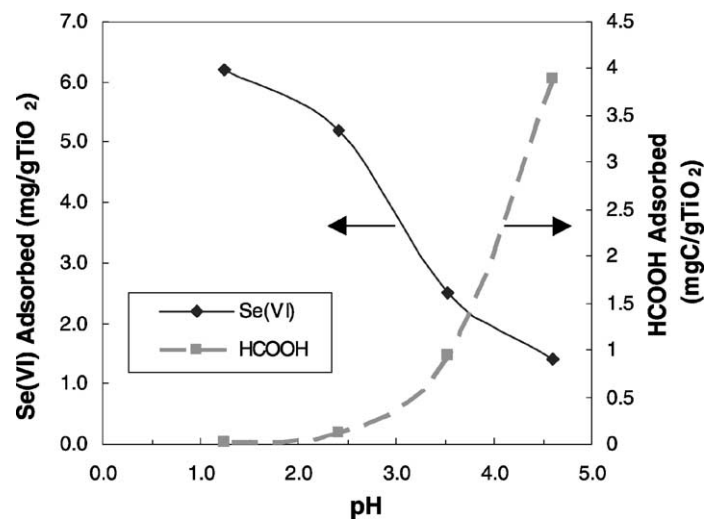

Fig. 5. The simultaneous adsorption of Se(VI) and HCOOH at various pH. Experimental conditions: 1 l test solution, $[Se(VI)]_0$: 20 ppm, $[HCOOH]_0$: 100 ppmC, 1.1 gTiO_2/l, N_2 purging, 293 K.

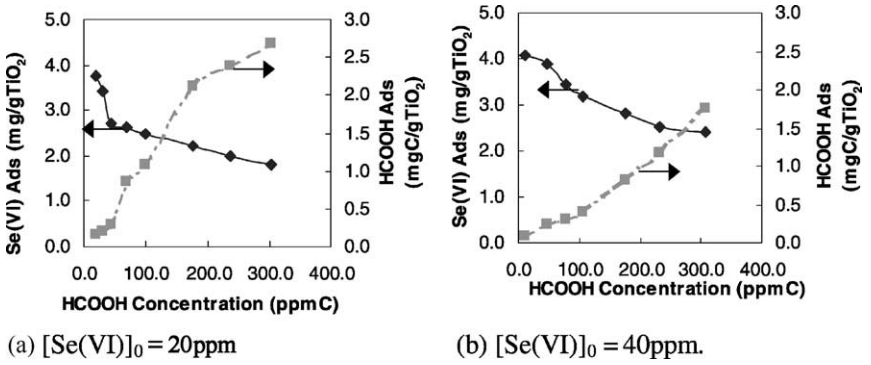

Fig. 6. Adsorption of Se(VI) and HCOOH at various initial HCOOH Concentration. Experimental conditions: pH 3.5, 1 l test solution, 1.1 gTiO_2/l, N_2 purging, 293 K.

formate:selenate ratio adsorbed onto the TiO_2 surface. The molar adsorption ratios were calculated to be 0.012, 0.152, 2.75 and 16.8 at the pH of 1.5, 2.5, 3.5 and 4.5, respectively. The relationship of these ratios and the photocatalytic reduction of Se(VI) will be discussed in the later sections.

The adsorption of Se(VI) and formic acid at different initial solute concentrations was also investigated. Fig. 6(a) and (b) shows the adsorption of Se(VI) and formic acid for an initial Se(VI) concentration of 20 and 40 ppm, respectively at varying formic acid concentrations. As the formic acid concentration increased, the amount of Se(VI) adsorbed decreased, showing the competitive adsorption of these two solutes.

3.2. Preliminary Se(VI) reduction studies

Preliminary studies of Se(VI) reduction were conducted in the presence and absence of UV irradiation and formic acid. The pH of the solution was 2.6 as a result of the 100 ppmC formic acid added in to the system. For experiments in which formic acid was not added, perchloric acid was used to adjust the pH to 2.6. This acid was used since perchlorate ions were found to have minimal impact on adsorption of other ions and photocatalysis [49]. The results are summarised in Table 1. In the absence of UV irradiation and formic acid (Experiment 1), about 28% of Se(VI) ions were removed from the solution and this was attributed to dark adsorption of the Se(VI) ions onto TiO_2 surfaces. A similar observation was encountered when formic acid was added to the solution in the absence of UV irradiation (Experiment 2) as well as in the presence of UV irradiation but with no formic acid added (Experiment 3).

When formic acid was introduced into the solution in the presence of UV irradiation (Experiment 4), about 92% of Se(VI) was removed from the solution after 60 min of irradiation. The colour of the test suspension changed from white to an intense orange due to the deposition of elemental Se on the TiO_2 surface,

Table 1
Preliminary experiments of Se(VI) reduction

Experiment	UV irradiation	Formic acid	Sparging gas	Se(VI) dark adsorption (%)	Total Se(VI) removed after illumination (%)	Colour change	H_2Se formed
1	No	No	N_2	28.0	28.0	No	No
2	No	Yes	N_2	27.0	27.0	No	No
3	Yes	No	N_2	26.9	26.9	No	No
4	Yes	Yes	N_2	26.9	91.6	Yes	Yes
5	Yes	Yes	Air	26.7	62.5	Yes	No

Experimental conditions: $[Se(VI)]_0$: 20 ppm (0.256 mM), $[HCOOH]_0$: 100 ppmC (8.3 mMC), 1 l test solution, pH = 2.6 ± 0.1, 1.1 g TiO_2/l, 293 K. Illumination time: Experiments 1 and 2: 30 min, Experiments 3–5: 60 min.

before changing back to white again due to the further photoreduction of Se to H_2Se. In the presence of formic acid, the photogenerated holes were effectively scavenged from the TiO_2 particles, preventing recombination with the photogenerated electrons and hence allowing electrons to reduce Se(VI) ions. This explained why Se(VI) reduction was not observed when formic acid was not added to the UV/TiO_2 system (in Experiment 3).

When the reaction suspension was sparged with air (see Table 1, Experiment 5), Se(VI) removal after 60 min was about 62%, as compared to 92% for the continuous nitrogen sparging experiment. It is postulated that the dissolved oxygen in the suspension competed with Se(VI) for the electrons, forming superoxide radical anions ($O_2^{\bullet -}$). This competition between oxygen and Se(VI) for electrons is believed to have impeded the reduction of Se(VI).

During the UV illumination of Se(VI)/TiO_2 suspension in the presence of formic acid, the following reactions are suggested to occur. In acidic solutions, Se(VI) can be reduced to Se(IV) and then to elemental selenium according to Eqs. (3) and (4), respectively [12]:

$$SeO_4^{2-} + 3H^+ + 2e^- \rightarrow ASeO_3^- + H_2O \quad (3)$$

$$HSeO_3^- + 5H^+ + 4e^- \rightarrow Se^0 + 3H_2O \quad (4)$$

Since Se(IV) ions were not detected in the bulk of the solution for all the experiments performed above, it is suggested that the Se(IV) ions were strongly adsorbed on the TiO_2 surface after being formed, and were subsequently reduced to elemental Se. The overall reduction of Se(VI) can then be written as Eq. (5):

$$SeO_4^{2-} + 8H^+ + 6e^- \rightarrow Se^0 + 4H_2O \quad (5)$$

The mineralisation of formic acid to carbon dioxide either by direct holes or hydroxyl radicals oxidation can be described by Eqs. (6a) and (6b), respectively:

$$HCOO^- + 2h^+ \rightarrow CO_2 + H^+ \quad (6a)$$

$$HCOO^- + OH^{\bullet} \rightarrow CO_2 + H_2O \quad (6b)$$

The formation of a black precipitate was started to appear in the clear-blue copper sulphate solution used as the hydrogen selenide trap when the most intense orange colour of the suspension was observed in the photoreactor. This corresponded to the near complete reduction of Se(VI) to elemental Se on the TiO_2 surface [42]. The black precipitate formed is believed to be copper (II) selenide (CuSe), although in this study, no test was done to confirm this as it had been confirmed in the literature [12,13]. The further reduction of elemental Se to H_2Se occurs according to Eq. (7):

$$Se^0 + 2H^+ + 2e^- \rightarrow H_2Se \quad (7)$$

A mass balance on Se (as shown in Table 2) confirmed the reduction of Se(VI) to elemental Se and the further reduction of elemental Se to H_2Se gas.

3.3. Effect of pH

Following the adsorption and the preliminary Se(VI) reduction experiments, the Se(VI) photoreduction reaction was studied at various pH values. The results presented in Fig. 7 shows the concentration profiles of Se(VI) as the photoreduction proceeded (following dark adsorption) at pH 2.2, 3.0 and 6.4. The initial Se(VI) concentration (at time: 0 min) is reflective of the Se(VI) dark adsorption. Se(VI) dark adsorptions at pH 2.2, 3.0 and 6.4 were 5.42, 3.68 and 0.12 mg/gTiO_2, respectively. These results consolidate the previously presented results that an increase in pH leads to a decrease in Se(VI) adsorption. Once the solution was exposed to UV illumination, the decrease in Se(VI) concentration was attributed to the reduction of Se(VI) to Se. From Fig. 7, the zero order rate represented the Se(VI) photoreduction rates well and hence was used for the rate estimation. Comparing the Se(VI) photoreduction rates at the different

Table 2
Mass balance of selenium species before and after photoreduction

Mass of Se added (mg)		Mass of Se after reduction (mg)			Error (%)
Se(VI) in suspension	Se(0) on TiO_2	Se(VI) in suspension	Se(0) on TiO_2	Se as H_2Se	
20.5	0	0.5	14.3	4.5	5.8

TiO_2 loading: 1.1 g/l, reaction volume: 1 l, residence time: 65 min, pH: 3.5.

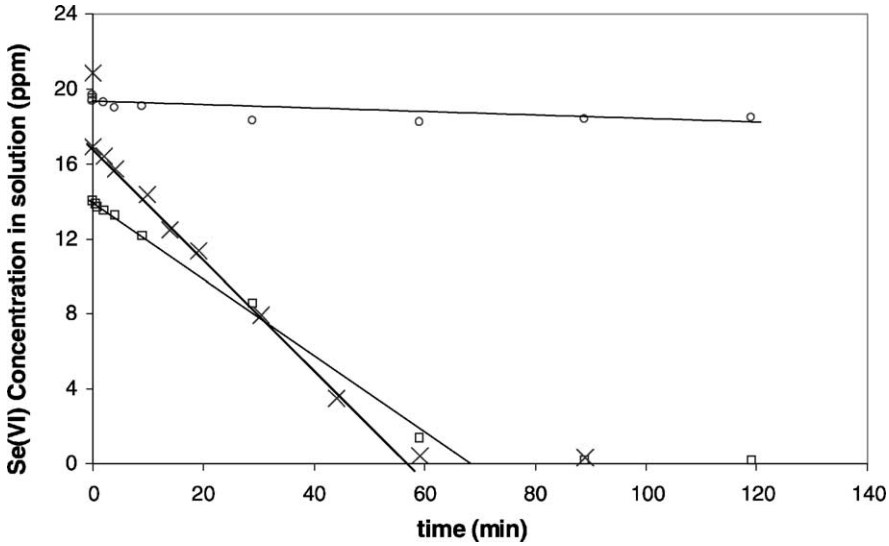

Fig. 7. Concentration profile of Se(VI) with time. Insert: experimental data fitted by zero order rate. (□) pH 2.2 ($R^2 = 0.996$), (×) pH 3.0 ($R^2 = 0.996$), (○) pH 6.4 ($R^2 = 0.854$). Experimental conditions: 1 l test solution, $[Se(VI)]_0$: 20 ppm, $[HCOOH]_0$: 100 ppmC, 1.1 gTiO_2/l, N_2 purging, 293 K, photon intensity 3.8 mmol/s.

pH values, it can be seen that the rate was the fastest at pH 3.0 and the slowest at pH 6.4.

In order to further evaluate the effect of pH, Se(VI) photoreduction experiments were carried out at other pH values. These results, presented as the Se(VI) photoreduction rates as a function of pH are shown in Fig. 8. The Se(VI) photoreduction rate increased and reached a maximum value at pH 3.5, followed by a decrease until the photoreduction ceased at pH 6.5. This observed trend can again be correlated with the effects of pH on Se(VI) and formate adsorption shown in Fig. 5. It is interesting to note that the observed rate peak at pH 3.5 corresponded to a formate-to-selenate molar ratio of 2.75. This is very close to the stoichiometry of 3:1 of the overall reaction as determined from balancing the number of e^- and h^+ generated in Eqs. (5) and (6a):

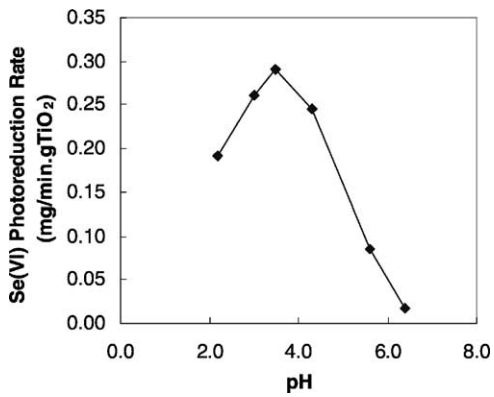

Fig. 8. The effect of pH on Se(VI) photoreduction rate. Experimental conditions: 1 l test solution, $[Se(VI)]_0$: 20 ppm, $[HCOOH]_0$: 100 ppmC, 1.1 gTiO_2/l, N_2 purging, 293 K, photon intensity 3.8 mmol/s.

$$3HCOO^- + SeO_4{}^{2-} + 5H^+ \rightarrow Se^0 + 4H_2O + 3CO_2 \quad (8)$$

This finding may be suggestive of the importance of a near stoichiometric adsorption of formate and Se(VI) ions on the TiO_2 surface in order to achieve the highest efficiency in capturing the photogenerated electrons and holes by Se(VI) and formate ions, respectively. The importance of stoichiometric adsorption is demonstrative that the redox reaction took place on the TiO_2 surface, of which the surface sites for the adsorption of both solutes could be limited. The limitation of surface sites was demonstrated earlier by the competitive adsorptions between the Se(VI) and formate ions.

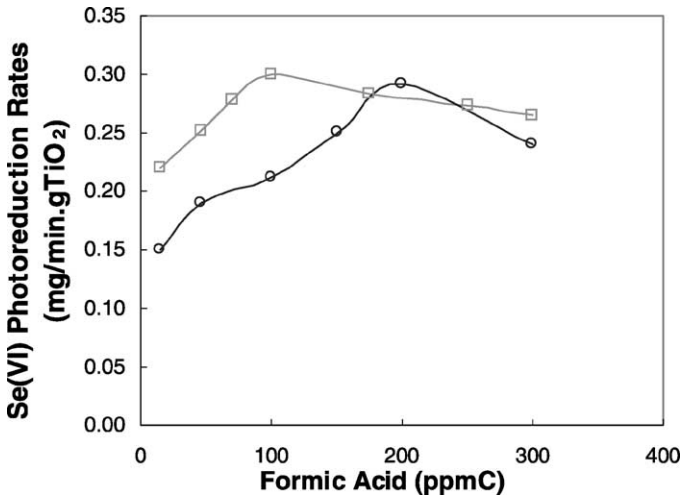

Fig. 9. The effect of initial HCOOH concentrations on Se(VI) photoreduction rates. Experimental conditions: pH 3.5, 1 l test solution, 1.1 gTiO_2/l, N_2 purging, 293 K.

3.4. Effects of initial solute concentration

In the next series of experiments, the effect of initial Se(VI) and formic acid concentrations on the Se(VI) photoreduction rates were studied. The experimental conditions were similar to those described earlier for the adsorption experiments (Fig. 6). The photoreduction results, represented by the zero order rates, are shown in Fig. 9. It can be observed from Fig. 9 that increasing the formic acid concentrations from 10 to 300 ppmC resulted in the increase in reduction rates until a maximum value was reached. Beyond this maximum value, a higher formic acid concentration was found to depress the reduction rate. The optimum formate ion concentrations corresponding with an initial Se(VI) concentration of 20 and 40 ppm were 100 and 200 ppmC, respectively. The adsorption tests (Fig. 6(a) and (b)) showed that as the formic acid concentration increased from 15 to 300 ppmC, Se(VI) adsorption onto TiO_2 surface decreased. From the adsorption data presented in Fig. 6(a) and (b), the formate:Se(VI) molar adsorption ratios for the two optimum conditions discussed above were 2.6 and 2.7. These two values are again comparable to the stoichiometric ratio of 3:1 in the reaction described in Eq. (8). Hence, the existence of an optimum formate ions concentration (as observed in Fig. 9) may also be attributed to the near 3:1 stoichiometric adsorption ratio of formate:Se(VI) ions, resulting in more efficient traps for both photogenerated electrons and holes. The same value for the maximum photoreduction rates of about 0.3 mg/min gTiO_2 obtained at 20 and 40 ppm Se(VI) concentration is also highly supportive of the occurrence of optimum conditions which closely corresponded to a stoichimetric adsorption ratio.

The maximum photoreduction rates were also manifested in the results of the investigations by Chenthamarakshan and Rajeshwar [50] during the photocatalytic reduction of chromate using TiO_2. In their study, it was found that by increasing the concentration of organic additives, even though the adsorption of chromate was decreased, the reduction rate was significantly enhanced, indicating the existence of an optimum organic concentration.. However, no explanation was provided as to why an optimum concentration existed [50].

3.5. Validation of the significance of optimum adsorption

To further validate the importance of stoichiometric adsorption, four different sets of adsorption and photoreduction experiments (Sets A–D) of different initial Se(VI) and formic acid concentrations. The experiments of Set A had initial Se(VI) and formic acid concentrations of 10 ppm and 50 ppmC, respectively,

Table 3
Effect of formate:Se(VI) molar adsorption ratio on Se(VI) photoreduction rate

pH	Adsorption experiments			Photoreduction experiments
	Se(VI) (mg/gTiO_2)	Formate (mgC/gTiO_2)	Formate:Se(VI) molar ratio	Se(VI) photoreduction rate (mg/min gTiO_2)
Set A				
3.5	1.91	0.102	0.351	0.229
3.9	1.62	0.211	0.856	0.253
4.4	0.851	0.432	3.32	0.303
4.8	0.301	0.502	11.0	0.263
Set B				
3.5	2.86	1.35	3.10	0.309
4.0	2.58	1.61	4.27	0.263
4.4	2.21	2.48	7.34	0.187

Experimental conditions for Sets A and B: 1 l test solution, 1.1 gTiO_2/l, 293 K, N_2 purging, 60 min residence time. Set A: $[Se(VI)]_0$: 10 ppm, $[HCOOH]_0$: 50 ppm, Set B: $[Se(VI)]_0$: 40 ppm, $[HCOOH]_0$: 200 ppm.

while those of Set B were 40 ppm and 200 ppmC, respectively. Experiment Sets A and B were carried out at various pH values. The results are summarised in Table 3.

By adjusting the pH of the solution, the amount of Se(VI) and the formate ions adsorbed onto the TiO_2 surface was varied. The two different starting initial reactant concentrations (i.e. the difference between Sets A and B) were used since this allowed for a wider range of adsorbed molar ratios of formate to Se(VI) ions. As can be seen from the presented results, when the adsorption of formate and Se(VI) ions was near the stoichiometric molar ratio, the optimum Se(VI) photoreduction rate was encountered. The optimum pH for Set A was found to be 4.4 while that of Set B was 3.5. Again, the maximum rates were also found to be close to the value of 0.3 mg/min gTiO_2, strongly supporting the existence of optimum conditions at a stoichiometric adsorption ratio.

Another sets of experiment (Sets C and D) were performed by varying the order of Se(VI) and formic acid addition into the TiO_2 suspension. The results are summarized in Table 4. These experiments were carried out at a different catalyst loading and reaction volume to test the validity of the above mentioned postulation under a different condition. The order of addition was as follows—Method 1: addition of formic acid and stirred for 30 min, followed by the addition of Se(VI) ions and stirred for 30 min, Method 2: addition of Se(VI) ions followed by the formic

Table 4
Effect of varying the order of Se(VI) and formic acid addition into the TiO_2 suspension

Method	Adsorption experiments			Photoreduction experiments
	Se(VI) (mg/gTiO_2)	Formate (mgC/gTiO_2)	Formate:Se(VI) molar ratio	Se(VI) photoreduction rate (mg/min gTiO_2)
Set C				
1	3.40	0.352	0.682	0.470
2	3.62	0.101	0.183	0.372
3	3.55	0.301	0.557	0.446
Set D				
1	2.52	1.21	3.16	0.588
2	3.18	0.542	1.12	0.492
3	2.61	1.11	2.79	0.593

Experimental conditions for Set C and D: pH 3.5, 0.5 l test solution, 0.5 g TiO_2/l, 293 K, N_2 purging, 60 min residence time. Set C: $[Se(VI)]_0$: 20 ppm, $[HCOOH]_0$: 20 ppmC, Set D: $[Se(VI)]_0$: 20 ppm, $[HCOOH]_0$: 100 ppmC.

acid, each stirred for 30 min and Method 3: simultaneous addition of both Se(VI) and formic acid and stirred for 30 min, followed by irradiation of the suspension. These experiments were performed based on the knowledge that Se(VI) ions have a stronger affinity to TiO_2 as indicated from the adsorption isotherms obtained earlier (Figs. 2 and 3). By subjecting TiO_2 to formic acid adsorption first, formate ions would have a greater chance of adsorption onto TiO_2 while Se(VI) could still probably be adsorbed when introduced later.

Both experiments of Sets C and D indicated that adsorbing formic acid first resulted in a higher Se(VI) photoreduction rate than by adsorbing Se(VI) first (compare Method 1 with 2 in Sets C and D). However, this was comparable to that of simultaneous adsorption (compare Method 1 with 3 in Sets C and D). This showed that Se(VI) ions have greater affinity to TiO_2. The results from Set D also indicated that the fastest rate also correlated well to stoichiometric adsorption ratio of 3:1. Comparing Sets C and D, increasing the initial formic acid concentration from 20 to 100 ppmC would increase the reduction rates. This shows that a high formic acid concentration was necessary to maintain a favourable formate adsorption.

4. Conclusions

The effects of pH and initial solute concentration (formic acid and Se(VI)) on the UV/TiO_2 reduction process of Se(VI) ions were investigated. It was found that the adsorption of both Se(VI) and formate ions onto the TiO_2 surface were essential for Se(VI) photoreduction to elemental Se. The photoreduction rate was depressed in the presence of oxygen. The elemental Se was further reduced to hydrogen selenide once the selenate ions were exhausted from the solution. The optimum Se(VI) photoreduction rate was found to be closely correlated to the molar adsorption ratio of approximately 3:1 of formate-to-selenate on the TiO_2 surface. This was suggested to be due to the limited surface sites as a result of competitive adsorption between Se(VI) and formate ions. It was possible to adjust the amount of formate and Se(VI) ions adsorbed onto the TiO_2 surface to its optimum ratio by changing the pH and initial solute concentration to obtain optimum Se(VI) photoreduction rate.

Acknowledgements

The author Timothy T.Y. Tan would like to acknowledge the Australian Institute of Nuclear Science and Engineering (AINSE) for financial support and The University of New South Wales and the Department of Education, Training and Youth Affairs DETYA) for awarding the International Postgraduate Research Scholarship. The authors would also like to thank Dr. Myint Zaw from the Australian Nuclear Science and Technology Organisation (ANSTO) for his assistance in the various aspects of this project.

References

[1] Y. Zhang, J.N. Moore, Environ. Sci. Technol. 30 (1996) 2613.
[2] Y. Zhang, J.N. Moore, Appl. Geochem. 12 (1997) 685.
[3] Agency for Toxic Substances and Disease Registry (ATSDR) Website, Retrieved 15 July 2002 (http://www.atsdr.cdc.gov/toxprofiles/phs92.html).
[4] H.M. Ohlendorf, D.J. Hoffman, M.K. Saiki, T.W. Aidrich, Sci. Total Environ. 52 (1986) 49–63.
[5] D. Wang, G. Alfthan, A. Aro, A. Makela, S. Knuuttila, T. Hammar, Agric. Ecosys. Environ. 54 (1995) 137.
[6] G.M. Peters, W.A. Maher, D. Jolley, B.I. Carroll, V.G. Gomes, A.V. Jenkinson, G.D. McOrist, Org. Geochem. 30 (1999a) 1287.
[7] G.M. Peters, W.A. Maher, F. Krikowa, A.C. Roach, H.K. Jeswani, J.P. Barford, V.G. Gomes, D.D. Reible, Mar. Environ. Res. 47 (1999) 491.
[8] P.H. Masscheleyn, R.D. Delaune, H.P. Patrick Jr., Environ. Sci. Technol. 24 (1990) 91.
[9] P. Zhang, D.L. Sparks, Environ. Sci. Technol. 24 (1990) 1848.
[10] M.A.R. Abdel-Moati, Estuar. Coast. Shelf Sci. 46 (1998) 621–628.
[11] M.J. Jones, R. French, Local Government Engineering in Australia, The Federation Press, Leichhardt, NSW, 1999, p. 141.
[12] S. Sanuki, T. Kojima, K. Arai, S. Nagaoka, H. Majima, Metall. Mater. Trans. B 30B (1999) 15.
[13] S. Sanuki, K. Shako, S. Nagaoka, H. Majima, Mater. Trans., JIM 41 (2000) 799.
[14] T.J. Sorg, G.S. Logsdon, J. Am. Water Works (1978) 379.
[15] A. Ramana, A. Sengupta, J. Environ. Eng. 118 (1992) 755.
[16] K.J. Gleason, in: R. Bartsch, J.D. Ways (Eds.), Chemical Separations with Liquid Membranes, American Chemical Society, Washington, DC, 1996, p. 342 (Chapter 24).
[17] Y.K. Kharaka, Appl. Geochem. 11 (1996) 797.
[18] M. Fujita, M. Lke, S. Nishimoto, K. Takahashi, M. Kashiwa, J. Ferment. Bioeng. 83 (1997) 517.
[19] C. Garbisu, T. Ishii, T. Leighton, B.B. Buchanan, Chem. Geol. 132 (1996) 199.
[20] D.T. Maiers, P.L. Wichlacz, D.L. Thompson, D.F. Bruhn, Appl. Environ. Microbiol. 54 (1988) 2591.

[21] M. Ike, K. Takahashi, T. Fujita, M. Kashiwa, M. Fujita, Water Res. 34 (2000) 3019.
[22] A. Murphy, Ind. Eng. Chem. Res. 27 (1988) 27 187.
[23] S.C.B. Myneni, T.K. Tokunaga, G.E. Brown Jr., Science 278 (1997) 1106.
[24] P. Refait, L. Simon, J.R. Genin, Environ. Sci. Technol. 34 (2000) 819.
[25] S.R. Qiu, H.F. Lai, J. Roberson, M.L. Hunt, C. Amrhein, L.C. Giancarlo, G.W. Flynn, J.A. Yarmoff, Langmuir 16 (2000) 2230.
[26] A. Fujishima, K. Hashimoto, T. Watanabe, in: D.A. Tryk (Ed.), TiO_2 Photocatalysis: Fundamentals and Applications, BKC INC, Japan, 1999, p. 124 (Chapter 8).
[27] W. Spacek, R. Bauer, G. Heisler, Chemosphere 30 (1994) 477.
[28] D. Chen, A.K. Ray, Chem. Eng. Sci. 56 (2001) 1561.
[29] M.I. Litter, Appl. Catal. B. 23 (1999) 89.
[30] M. Alam, R.A. Montalvo, Metall. Mater. Trans. B 29B (1998) 95.
[31] G.D. Surender, G.P. Fotou, S.E. Pratsinis, Trends Chem. Eng. 4 (1998) 145.
[32] R. Terzian, N. Serpone, C. Minero, E. Pelizzeyyi, J. Catal. 128 (1991) 352.
[33] M.R.V. Sahyun, N. Serpone, Langmuir 13 (1997) 5082.
[34] C. Xi, Z. Chen, Q. Li, Z. Jin, J. Photochem. Photobiol. A 78 (1995) 249.
[35] Y. Ku, I. L Jung, Water Res. 35 (2001) 135.
[36] J.A. Navio, G. Colon, M. Trillas, J. Peral, X. Domenech, J.J. Testa, J. Padron, D. Rodriguez, M.I. Litter, Appl. Catal. B 16 (1998) 187.
[37] B. Bems, F.C. Jentoft, R. Schlogl, Appl. Catal B 20 (1999) 115.
[38] A. Kudo, K. Domen, K. Maruya, T. Onishi, J. Catal. 135 (1992) 300.
[39] C.R. Chenthamarakshan, H. Yang, Y. Ming, K. Rajeshwar, J. Electroanal. Chem. 494 (2000a) 79.
[40] C.R. Chenthamarakshan, K. Rajeshwar, Electrochem. Comm. 22 (2000) 527.
[41] M.R. Prairie, L.R. Evans, B.M. Stange, S.L. Martinez, Environ. Sci. Technol. 27 (1993) 1776.
[42] E. Kikuchi, H. Sakamoto, J. Electrochem. Soc. 147 (2000) 4589.
[43] C.G. Hatchard, C.A. Parker, Proc. R. Soc. (1956) 518.
[44] N.J. Bruce, in: J.C. Scarano (Ed.), CRC Handbook of Organic Photochemistry, vol. 1, CRC Press, Boca Raton, FL, 1989, p. 241 (Chapter 9).
[45] K.M. Holtzclaw, R.H. Neal, G. Sposito, S.J. Traina, Soil Sci. Soc. 51 (1987) 75.
[46] S.J. Gregg, K.S.W. Sing, in: Adsorption, Surface Area and Porosity, second ed., Academic Press, London, UK, 1982, p. 41 (Chapter 2).
[47] F. Seby, M. Potin-Gautier, E. Giffaut, G. Borge, O.F.X. Donard, Chem. Geol. 171 (2001) 173.
[48] R. Chang, in: Chemistry, fifth ed., McGraw-Hill, 1994, p. 633 (Chapter 16).
[49] M. Abdullah, G.K.C. Low, R.W. Matthews, J. Phy. Chem. 94 (1990) 6820.
[50] C.R. Chenthamarakshan, K. Rajeshwar, Langmuir 16 (2000) 2715.